Development of an Innovative Magnetorheological Fluids-based Haptic Device Excited by Permanent Magnets*

Claudia Simonelli, Antonino Musolino, Rocco Rizzo, and Lynette A. Jones, *Fellow, IEEE*

***Abstract*— A number of haptic displays based on smart fluidic materials such as electrorheological (ERFs) and magnetorheological fluids (MRFs) have been fabricated. These displays are relevant to medical virtual environments where it is important to create realistic simulations of soft tissues with varying stiffness. In this paper a new haptic device is described that was designed in consideration of the limitations of an earlier MRF display. The new prototype consists of 400 permanent magnets (PMs) arranged in a 20x20 array that is underneath a chamber filled with MRF. The magnetic field within the fluid is controlled by 400 PM stepping motors that move the magnets vertically. The magnetic behavior of the device was simulated using FEM which indicated that its spatial resolution was substantially improved when compared to the earlier prototype and that objects as small as 10 mm can be rendered. The device was fabricated and assembled and measurements demonstrated the accuracy of the FE model. Its novelty is demonstrated by the increased intensity of the magnetic field produced and the enhanced spatial resolution. These features will enable the dynamic presentation of haptic information such as object shape and compliance which will be characterized in future psychophysical experiments.**

I. Introduction

A range of actuator technologies have been used to create haptic displays including electromagnetic, pneumatic, ultrasonic, piezoelectric, and shape memory alloy [1-3]. Electromagnetic and piezoelectric actuators are the most extensively used due to their compact size, low cost and ease of control. Displays based on these actuators typically vibrate the skin to alert the user or convey information about the spatial features of the environment (e.g., virtual textures, collision avoidance systems in vehicles). There are a number of applications of haptic displays for which vibration is limited in its capacity to render the properties of interest. For example, in medical and surgical virtual environments it is important to create realistic simulations of soft tissues with varying stiffness [4]. Since tumors are stiffer than healthy tissue, haptic displays that can render such stiffness distributions are essential to their use in devices that palpate tissue as part of the diagnostic process. To address this need, haptic displays based on smart fluidic materials such as electrorheological (ERFs) and magnetorheological fluids (MRFs) have been explored [5-7]. MRFs are suspensions of micron-sized ferrous particles in oil that exhibit a rapid and reversible transition from a liquid state to a near-solid state when an external magnetic field is applied (see Figure 1.). MRF actuators are particularly suitable for haptic interfaces because of their high yield stress, low mass-torque and inertia-torque ratios, fast response times, and the simplicity of their excitation system [8-10].

A number of MRF-based haptic displays have been developed and tested in applications ranging from simulating the mechanical properties of biological tissues [11] to rendering the 2D shapes of objects [7, 12]. There has also been some recent work on embedding compact MRF actuators in shoes, where they are used to create virtual surface deformations that the user experiences while walking in a virtual environment [13]. The mode of interaction between the user and the MRF-based haptic display in these applications has varied. Typically, the MRF is encapsulated and users move their fingers across a membrane to perceive the presence of a stiff region. A number of tactile elements may comprise the display which enables the stiffness of individual units in the array to be controlled [5, 14]. With larger displays the MRF is usually manually explored with a gloved hand and the task for the user is to identify different shapes rendered in the MRF or to locate regions of higher stiffness [12, 15].

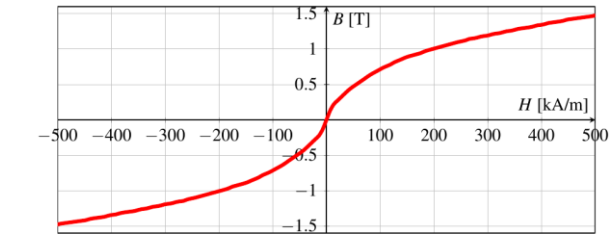

a) BH curve

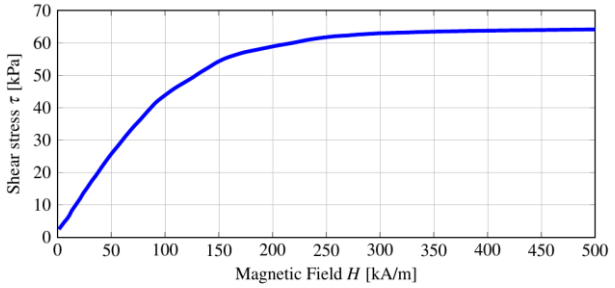

b) tauH curve

Figure 1. (a) Magnetic and (b) mechanical properties of MRF-140CG.

* Research supported by the University of Pisa, within the framework of MIT-UNIPI project, COAN CA 4.002.03.03 and the US National Science Foundation

C. Simonelli, A. Musolino, and R. Rizzo are with the Department of Engineering for Energy and Systems, University of Pisa, Italy (e-mail: claudia.simonelli@phd.unipi.it, antonino.musolino, rocco.rizzo@unipi.it).

L. A. Jones is with the Department of Mechanical Engineering, Massachusetts Institute of Technology, Cambridge, MA 02139, USA (e-mail: ljones@MIT.edu).

II. PREVIOUSLY DEVELOPED PROTOTYPES

Several MRF-based haptic displays have been developed and tested over the years at the University of Pisa with the objective of evaluating their ability to render shapes that are manually explored and identified. The devices enabled unconstrained exploration and direct contact with the objects presented. These displays have also provided an interface for understanding fundamental properties of human haptic perception [7, 9, 12, 15, 16].

The Haptic Black Box (HBB-I) prototype comprised 16 solenoids arranged in a 4x4 configuration that formed the excitation system. These were placed underneath a 200 mm x 200 mm square plexiglass chamber containing the MRF (see Figure 2). The magnetic field inside the chamber was controlled by varying the current flowing in the coils. By controlling the current delivered to the coils virtual objects could be created within the fluid with a given shape and compliance. The MRF used in this device was MRF-140CG (Lord Corporation®, Cary NC, USA).

A 3D Finite Element (FE) analysis, performed with the FEM code EFFE [17], highlighted that the flux density amplitude decreased to low values just outside the coil base, and at a distance of 10 mm from the chamber, the field was attenuated by about 65%. The presence of this magnetic field gradient meant that the edges of virtual objects within the MRF were attenuated.

Several psychophysical tests were performed using this prototype to evaluate its capacity to render shapes of varying dimensions. Each participant sat in front of the haptic device without seeing the chamber and with a glove on their preferred hand they explored the fluid [12]. In a shape recognition test, fifteen participants moved their hand through the MRF until they could identify which of ten different shapes was presented. Their overall performance was good with a group mean score of 73% correct. A further experiment determined the spatial resolution of the haptic device by measuring the accuracy with which participants could localize a stiff region within the MRF. In this task the group mean score was 86% correct. It was noted, however, that stimuli presented near the edges of the display were easier to locate than those in the middle [12].

Figure 2. HBB-I prototype and excitation system: the current produced by the four-by-four array of solenoids produces the magnetic field [12].

A. *Critical issues*

The tests performed on the HBB-I demonstrated the feasibility of using the display to present various shapes but also highlighted some limitations of this prototype. The spatial resolution of the display was low due to the distance (about 47 mm) between neighboring coils which constrained the minimum size of virtual objects that could be created within the fluid (about 20 mm, corresponding to the cores' diameter). The magnetic field within the MRF was also relatively low at 0.25 T and the efficiency of the excitation system was about 14%.

III. NEW HAPTIC DEVICE

Based on the analysis of the critical issues associated with the HBB-I, a new haptic interface called the Haptic Black Box-with Permanent Magnet device (HBB-PM) has been designed and fabricated. The excitation system of the HBB-I prototype has been replaced to improve the performance of this device. This new prototype consists of 400 permanent magnets (PMs) arranged in a 20x20 array that is placed underneath the chamber filled with the MRF. The NdFeB magnets have a remanence of about 1.4 T. The dimensions of each magnet are 10x10x10 mm, and the distance between two adjacent PMs is 3 mm. It is possible to control the magnetic field within the fluid using an actuation system, which consists of 400 PM stepping motors, that move the magnets in the vertical direction.

A. *Finite Element Analysis*

The magnetic behavior of the device was simulated using a FE model created in EFFE (see Figure 3). We evaluated the field inside the fluid activating one or more PMs, in order to show the feasibility of creating shapes in the chamber.

For example, in Figure 4 a hemisphere in the chamber was created by activating a single PM. Figure 5 shows an additional simulation when four adjacent PMs are activated. This configuration can create an L-shape inside the fluid. In both the figures the results in terms of magnetic flux density are shown, and the arrangement of the PMs in the x-y plane are highlighted in the background in order to identify which PMs are activated below the fluid chamber.

Finally, Figure 6 shows a more complex shape which the HBB-PM device can create inside the fluid.

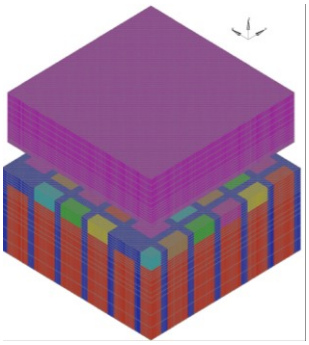

Figure 3. Finite element simulated model of HBB-PM device.

Figure 7 shows the actuation force required to raise a single magnet as a function of the distance between the chamber and the PM itself, derived from the simulation results. The distance is at a minimum when the PM is in contact with the chamber and increases when the PM is retracted. The distance between a PM and the chamber was varied, and the actuation force obtained; it was denoted as positive when the PM was pushed upward. Based on these results, we determined the actuators that would be required to move the PMs.

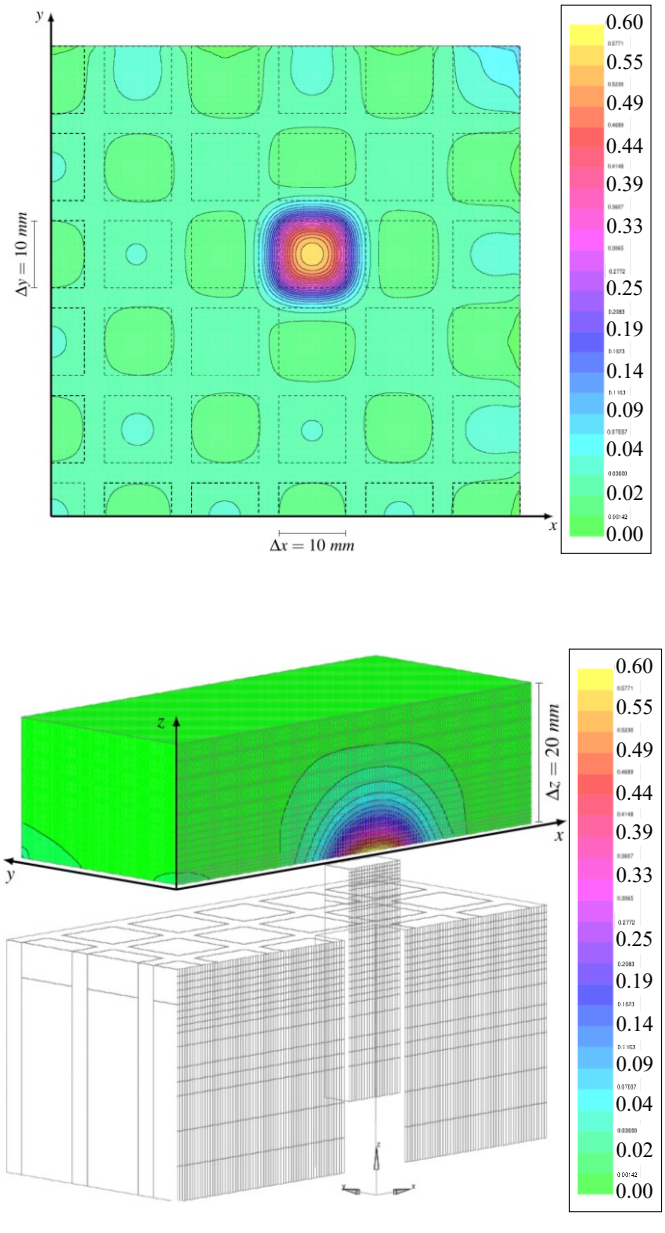

Figure 4. Simulation of the particular condition in which a single PM is in contact with the base of the box. 2D and 3D views. Values of field are expressed in Tesla (T).

We then simulated the magnetic induction distribution along a line in the center of a PM. We evaluated the field at 2 mm from the bottom of the chamber, varying the distance between a PM and the chamber in 1 mm steps. The spatial distribution of the magnetic induction produced by a single PM is illustrated in Figure 8. All the PMs are aligned at 10 mm from the MRF chamber in all the simulations, whereas they were placed at 20 mm in the final prototype.

Based on the simulation results, the spatial resolution of the new device is substantially better than that of HBB-I (13 mm as compared to 47 mm). In addition, the new actuation system enables objects as small as 10 mm to be rendered in the MRF. The spatial resolution is related to the dimensions of the excitation system (i.e., the PMs' dimensions), considering that the MR fluid starts its transition from a liquid state to semi-solid when the magnetic flux density is above 0.15-0.2 Tesla. Furthermore, as described in [18] and [19] when an operator's fingers "squeeze" a portion of excited fluid, the field is concentrated in a narrower space, which has an area about the same as that of the PM. The intensity of the magnetic field inside the fluid has also increased to around 0.45 T, and the efficiency of the excitation system for the display has improved by approximately 70%.

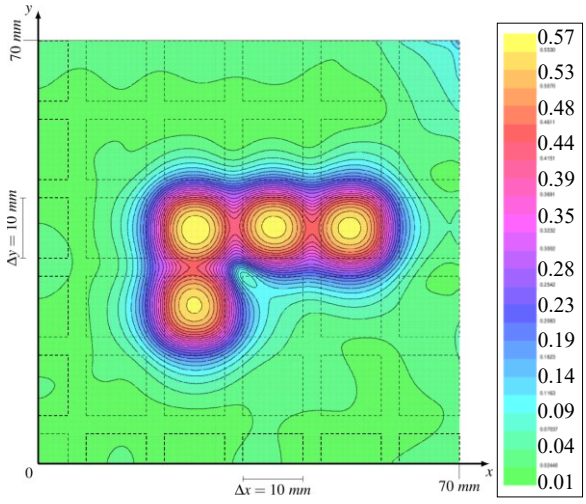

Figure 5. Simulation of an L-shape rendered within the fluid. Values of the field are expressed in Tesla (T). In the background, it is possible to identify all the PMs' positions below the fluid chamber.

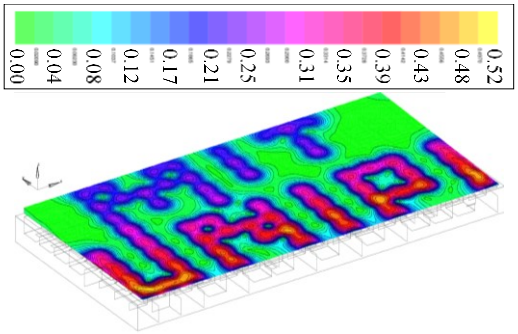

Figure 6. Simulation of an example that shows how shapes can be rendered within the fluid. Values of field are expressed in Tesla (T).

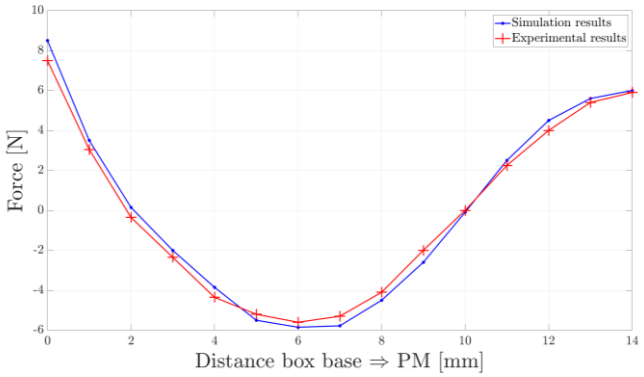

Figure 7. Force amplitude as a function of the distance between the PM and the chamber base. The distance is at a minimum when the magnet is in contact with the bottom of the chamber and it increases when the magnet is retracted. The force is positive when the PM is pushed upward. All the PMs are aligned at 10 mm from the MRF chamber.

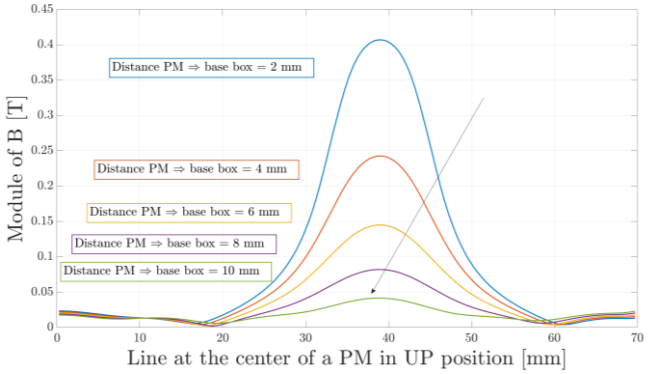

Figure 8. Spatial distribution of magnetic induction. Each curve is derived at a fixed distance that changes in 2 mm steps. The maximum magnetic induction is reached when the PM is in contact with the base of the chamber. Simulation results.

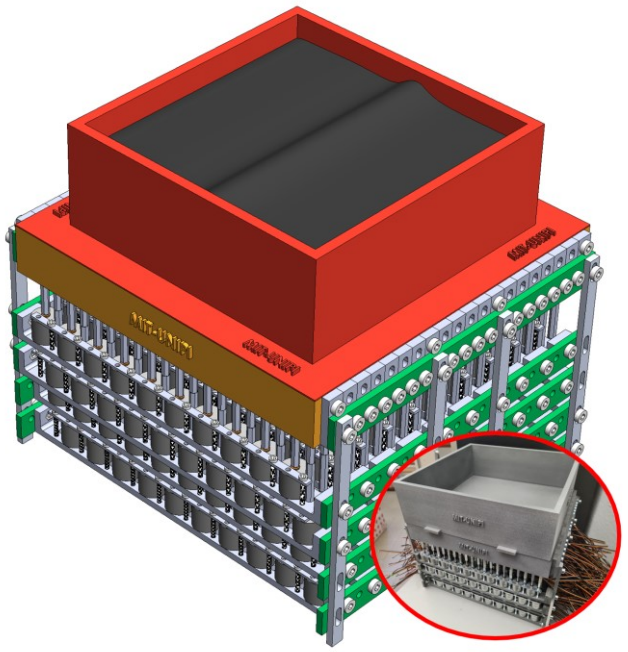

Figure 9. Assembly design of the HBB-PM and the prototype.

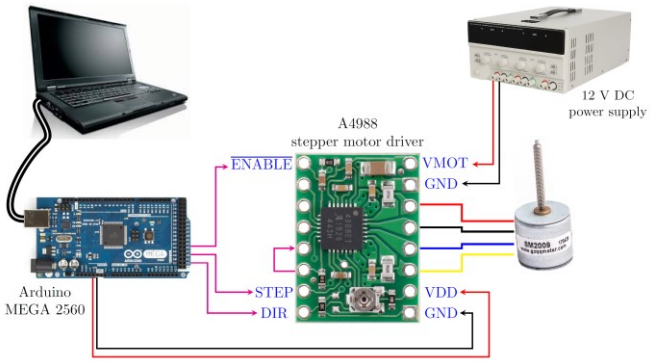

Figure 10. Control system scheme of a single actuator.

B. *Design of the prototype*

We designed and built a full-scale prototype of HBB-PM, and determined the correct positioning of all the elements using 3D CAD software and placing the actuators below the chamber at different heights (see Figure 9). Most of the parts were 3D printed with the additive manufacturing process of Multi Jet Fusion (MJF), including the liquid-containing chamber for the MRF.

C. *Control system*

A position open-loop control system was chosen for this device. The excitation system relies on 400 actuators, each of which has to move a single PM. Each actuator receives the control signal from an Arduino board connected to the motor driver, and the power comes from a 12 V DC power supply. The applied load determines the actuator speed, and when there is no power, the actuator holds its position unless the load exceeds the back-drive force (see Figure 10).

D. *Preliminary electromagnetic validation tests*

In order to validate the FEM model, some preliminary measurements were made of the field and the force generated by the new display. Since it is not possible to experimentally measure the magnetic field inside the MRF without altering the flux lines, we evaluated the magnetic field in the free space (that is in the chamber without the MRF). We performed several measurements of the magnetic field in air (without the fluid) using a portable Gauss-meter equipped with a Hall sensor on a grid of points obtained by varying the x-y-z position. The maximum error between measured data and FEM results under the same conditions was less than 10% (see Figure 11). Furthermore, the goodness of fit of the FEM model was evaluated by measuring the actuation force required to separate a PM from the chamber containing the fluid using a commercial load cell with a 0-50 N measuring range (see Figure 12). All the PMs were placed at about 10 mm from the MRF

chamber, and a single PM was actuated. We varied the distance between the actuated PM and the chamber in 1 mm steps, while measuring the force. For this measurement, the difference between the actual value and simulated results was 12% (see Figure 7). In general, these preliminary measurements from the new display demonstrate that the simulation results are accurate.

Finally, the L-shape simulated in Figure 5 was created within the fluid as shown in Figure 13 to verify the operation of the HBB-PM display.

Figure 11. Preliminary measurements of the magnetic field in air (about 10 mm above the magnet) with a portable Gauss-meter F.W. Bell/4048 equipped with a Hall sensor.

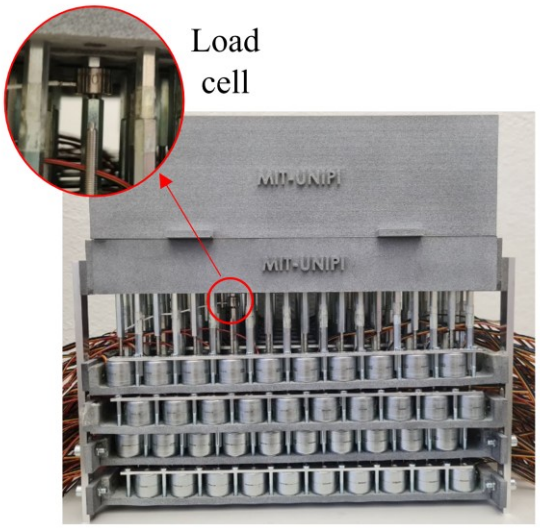

Figure 12. Preliminary test to determine the actuation force required to separate a PM from the base of the chamber containing the fluid.

Figure 13. Preliminary test to create an L-shape within the fluid.

IV. Future Studies

Future work will involve psychophysical tests with the HBB-PM haptic interface. Initially, its performance will be compared to that of the HBB-I prototype using shape recognition and localization tests. These will be conducted after further characterization of the HBB-PM device. In particular, the spatial resolution of the device will be measured so that the spatial dimensions of shapes that can be rendered within the fluid is known. The compliance of rendered shapes will also be measured. A map of the shear stress will be derived from simulations and experimental observations in order to determine how many PMs are required to create a region with the same spatial dimensions as the one presented in the HBB-I device when a single coil is excited. Once this has been determined, the performance of participants when localizing regions of enhanced stiffness and recognizing shapes in the new device can be meaningfully compared to that on the HBB-I device. Two new psychophysical tests have been designed to evaluate other aspects of the haptic interface.

A. Compliance discrimination test

The focus of this experiment is to test the capacity of participants to discriminate different compliances. The compliance of standard stimulus will be compared to those of a set of comparison stimuli using the method of constant stimuli. The compliance will be varied by controlling the gap between the PMs and the chamber, thereby adjusting the intensity of field within the fluid. On each trial, participants will judge which of two stimuli presented sequentially is the stiffer.

B. Dynamic test

In the dynamic test, the accuracy in identifying the direction of movement of a rendered shape in the display will be assessed. Participants will place their gloved hand resting palm down in the display while an array of 4x4 PMs will be sequentially activated. Different columns and rows of PMs will be activated and participants will be required to indicate the direction of movement. By varying both the temporal and spatial aspects of the stimuli presented it will be possible to derive benchmarks of the spatial and temporal resolution of the display.

V. Conclusions

An innovative magnetorheological fluids-based haptic device has been designed based on the limitations of an existing MRF haptic display. A reduced-scale prototype was assembled, and measurements showed the accuracy of the FE model. Then a full-scale prototype was designed and fabricated using the MJF 3D printing process. A preliminary set of measurements of the forces and magnetic fields generated by the device are consistent with those derived in the simulations. This display offers the intriguing possibility of creating dynamically varying shapes with changeable compliance that are perceived through manual exploration of a viscous medium.

Future studies will involve the complete electromagnetic validation of the system and the execution of psychophysical tests. The results from the psychophysical tests with the new haptic device should enhance our understanding of human stiffness perception and importantly indicate whether this changes when sensing occurs in a fluidic medium.

References

[1] J. C. Gwilliam, M. Bianchi, L. K. Su, and A. M. Okamura, "Characterization and psychophysical studies of an air-jet lump display," *IEEE Trans. Haptics*, vol. 6, pp. 156-166, 2013.

[2] V. Lévesque, J. Pasquero, V. Hayward, and M. Legault, "Display of virtual Braille dots by lateral skin deformation: Feasibility study" *ACM Trans. Appl. Perc*., vol. 2, pp. 132-149, 2005.

[3] M. Nakamura and L. Jones, "An actuator for the tactile vest – a torso-based haptic device. *11th Int. Symp. Haptic Interfaces Virt. Environ. Teleop. Sys.*, pp. 333-339, 2003.

[4] N. Najmaei, A. Asadian, M. R. Kermani, and R. V. Patel, "Performance evaluation of magneto-rheological actuation for haptic feedback in medical applications," *IEEE Int. Conf. Intell. Robot Sys.*, pp. 573-578, 2015.

[5] H. Ishizuka and N. Miki, "Miniature tactile elements for tactile display with high stiffness resolution with magnetorheological fluid," *IEEE Int. Conf. Micro-electro Mech. Sys*., pp. 1165-1168, 2016.

[6] H. Qin, A. Song, Z. Gao, Y. Liu, and G. Jiang, "A multi-finger interface with MR actuators for haptic applications," *IEEE Trans. Haptics,* vol. 11, pp. 5-14, 2018.

[7] N. Sgambelluri, E. P. Scilingo, R. Rizzo, and A. Bicchi, "A free-hand haptic interface based on magnetorheological fluids," in *The Sense of Touch and its Rendering,* STAR 45, A. Bicchi et al. (Eds), Berlin: Springer, 2008, pp. 155-178.

[8] R. Rizzo, "A permanent-magnet exciter for magneto-rheological fluid-based haptic interfaces," *IEEE Trans. Magnetics*, vol. 49, pp. 1390-1401, 2013.

[9] R. Rizzo, N. Sgambelluri, E. P. Scilingo, M. Raugi, and A. Bicchi, "Electromagnetic modeling and design of haptic interface prototypes based on magnetorhelogical fluids," *IEEE Trans. Magnetics*, vol. 43, pp. 3586-3600, 2007.

[10] N. Najmaei, M. R. Kermani, and R. V. Patel, "Suitability of small-scale magnetorheological fluid-based clutches in haptic interfaces for improved performance," *IEEE/ASME Trans. Mechatronics,* vol. 20, pp. 1863-1874, 2015.

[11] C. -H. Lee and M. -G. Jang, "Virtual surface characteristics of a tactile display using magneto-rheological fluids," *Sensors*, vol. 11, pp. 2845-2856, 2011.

[12] R. Rizzo, A. Musolino, and L. A. Jones, "Shape localization and recognition using a magnetorheological-fluid haptic display," *IEEE Transactions on Haptics*, vol. 11, no. 2, pp. 317-321, 2018.

[13] T. -H. Yang, H. Son, S. Byeon, H. Gil, I. Hwang, G. Jo, S. Choi, S, -Y. Kim, and J. R. Kim, "Magnetorheological fluid shoes for walking in VR," *IEEE Trans. Haptics*, accepted for publication.

[14] H. Ishizuka, N. Lorenzoni, and N. Miki, "Tactile display for presenting stiffness distribution using magnetorheological fluid," *JSME Mech. Eng. J*., vol. 1, 4, paper no. 14-00065, 2014.

[15] R. Rizzo, A. Musolino, M. Tucci, and L. A. Jones, "Displaying shape haptically using MRF-based device," *Proc. IEEE Eng. Med. Biol. Conf*., pp. 1164-1167, 2015.

[16] A. Bicchi, M. Raugi, R. Rizzo, and N. Sgambelluri, "Analysis and design of an electromagnetic system for the characterization of magneto-rheological fluids for haptic interfaces," *IEEE Trans. Magnetics,* vol. 41, pp. 1876-1879.

[17] EFFE, "Effe v2.00, user manual," Bathwick Electrical Design Ltd, 2009.

[18] N. Sgambelluri, E. P. Scilingo, A. Bicchi, R. Rizzo and M. Raugi, "Advanced modelling and preliminary psychophysical experiments for a free-hand haptic device," 2006 IEEE/RSJ International Conference on Intelligent Robots and Systems, 2006, pp. 1558-1563.

[19] R. Rizzo, "A Permanent-Magnet Exciter for Magneto-Rheological Fluid-Based Haptic Interfaces," in IEEE Transactions on Magnetics, vol. 49, no. 4, pp. 1390-1401, April 2013.